Structure, antiferromagnetism and superconductivity of the layered iron arsenide NaFeAs

Dinah R. Parker, Michael J. Pitcher, Peter J Baker, Isabel Franke, Tom Lancaster, Stephen J. Blundell and Simon J. Clarke*

Electronic Supplementary Information. Communication B818911K

Table S1. Summary of refinement of NaFeAs against Powder Neutron Diffraction (PND) data at 295 K, measured on the POLARIS instrument, ISIS facility, UK.

Space Group	*P*4/*nmm*
a / Å	3.9494(2)
c / Å	7.0396(8)
V / Å^3	109.804(1)
R_{wp}	0.0209
χ^2	1.523

Table S2. Refined atomic parameters for NaFeAs at 295 K, from data measured on the POLARIS instrument, ISIS facility, UK.

Atom	Site	*x*	*y*	*z*	U_{equiv} / Å^2 × 100
Fe	2*a*	0.75	0.25	0	0.66(1)
Na	2*c*	0.25	0.25	0.64602(7)	1.31(1)
As	2*c*	0.25	0.25	0.20278(3)	0.67(1)

Table S4. Refined anisotropic displacement parameters for NaFeAs from data measured at 295 K on the POLARIS instrument, ISIS facility, UK.

Atom	$U_{11} = U_{22}$ /Å^2 × 100	U_{33} / /Å^2 × 100
Fe	0.546(5)	0.899(8)
Na	1.315(9)	1.317(9)
As	0.577(7)	0.856(8)

Table S5. Summary of refinement of NaFeAs against Powder Neutron Diffraction (PND) data at 2.5 K, measured on the POLARIS instrument, ISIS facility, UK.

Space Group	*P*4/*nmm*
a / Å	3.94729(2)
c / Å	6.99112(6)
V / Å^3	108.930(1)
R_{wp}	0.0129
χ^2	1.598

Table S6. Refined atomic parameters for NaFeAs at 2.5 K, from data measured on the POLARIS instrument, ISIS facility, UK.

Atom	Site	*x*	*y*	*z*	U_{equiv} / Å^2 × 100
Fe	2*a*	0.75	0.25	0	0.19(1)
Na	2*c*	0.25	0.25	0.64673(8)	0.54(3)
As	2*c*	0.25	0.25	0.20234(4)	0.22(2)

Table S7. Refined anisotropic displacement parameters for NaFeAs from data measured at 2.5 K on the POLARIS instrument, ISIS facility, UK.

Atom	$U_{11} = U_{22}$ /Å^2 × 100	U_{33} / /Å^2 × 100
Fe	0.134(4)	0.317(8)
Na	0.429(9)	0.753(9)
As	0.184(7)	0.298(9)

Table S8. Refined bond lengths (Å) and angles (degrees) for NaFeAs at 295 K and 2.5 K from data measured on the POLARIS instrument, ISIS facility, UK.

	295 K	2.5 K
Fe–As [4][a]	2.4366(5)	2.4281(2)
Na–As [4]	2.9886(7)	2.9842(2)
Na–As [1]	3.1203(9)	3.1063(6)
Fe–Fe [4]	2.7927(7)	2.79115(3)
Na–Fe [4]	3.1795(7)	3.1620(5)
Na-Na [4]	3.4678(9)	3.4633(7)
As–Fe–As [2]	108.27(2)	108.74(1)
As–Fe–As [4]	110.07(1)	109.837(6)
As–Na–As [4]	82.713(8)	82.808(8)
As–Na–As[4]	110.86(1)	110.72(1)

[a] The number in square brackets indicates the number of symmetry equivalent bond lengths and angles

Figure S1. Rietveld refinements for NaFeAs at 2.5 K, measured on the POLARIS instrument, ISIS, UK. 145º bank. (note: peaks at ~ 2.1 Å from vanadium sample holder and cryostat)

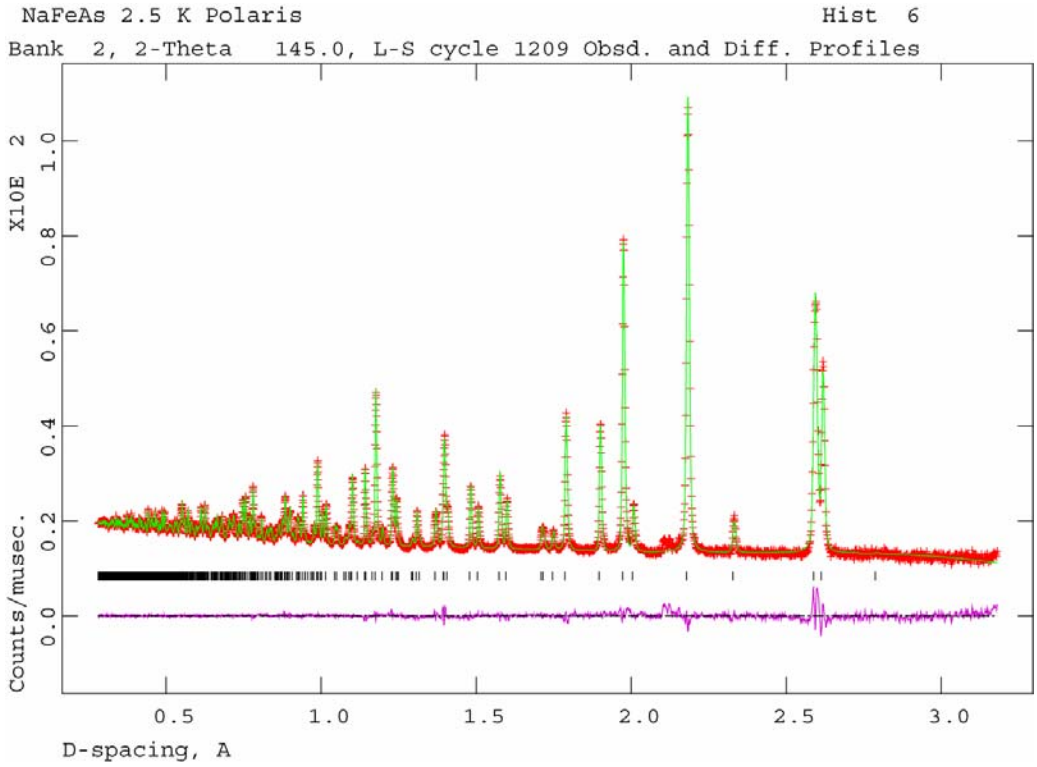

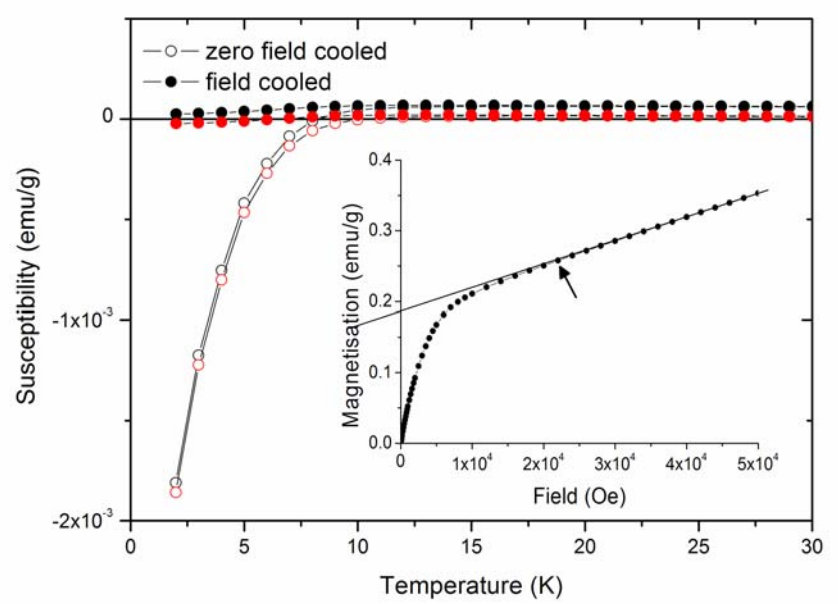

Fig. S2 Zero-field-cooled (ZFC) (black open circles) and field-cooled (FC) (black closed circles) susceptibilities versus temperature for NaFeAs measured in an applied field of 50 Oe (red open and closed circles show the ZFC and FC curves corrected for a Fe impurity of ~0.08% by mass); Inset: Magnetisation versus applied field of NaFeAs at 300 K.

Correction of the susceptibility data for a small elemental iron impurity. The plot of magnetisation versus applied field at 300 K, (Fig. S2, inset) reveals the presence of 0.08 % by mass of metallic Fe deduced from the saturation field ($H_{sat(Fe)} \approx 2.2 \times 10^4$ Oe) and saturation magnetisation of Fe (222 emu g^{-1}). This level of impurity is much smaller than can reasonably be detected by diffraction methods. Correcting for this impurity using the measured susceptibility of iron under the conditions used for measuring the NaFeAs sample (Fig. S2, red symbols) reveals a diamagnetic field-cooled susceptibility at low temperature. Note that this small amount of elemental iron is not sufficient to account for the small value of the diamagnetic signal. The corrected values are used in Figure 3 of the main article.

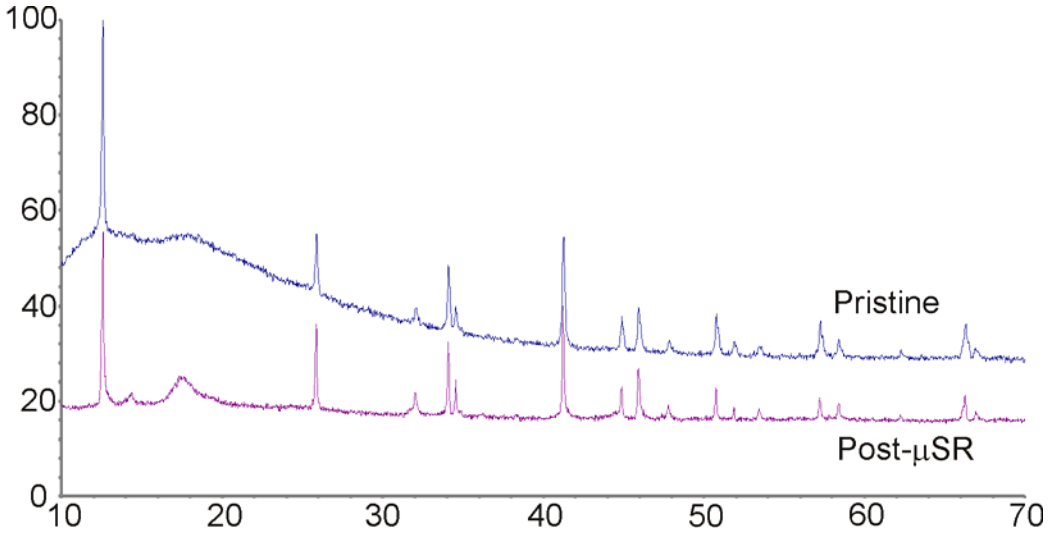

Fig. S4. Comparative X-ray diffractograms of the sample in its pristine state and after return to the laboratory after the μSR experiment. The broad features between 15 and 20 degrees in both diffractograms arise from the air-tight sample holder. The susceptibilities are compared in Figure 3 in the main text.